Experimental and Theoretical Studies of the d^8-d^{10} Interaction between Pd(II) and Au(I): Bis(chloro[(phenylthiomethyl)diphenylphosphine]gold(I))−dichloropalladium(II) and Related Systems

Olga Crespo and Antonio Laguna*,†

Departamento de Química Inorgánica, Instituto de Ciencia de Materiales de Aragón, Universidad de Zaragoza-CSIC, E-50009 Zaragoza, Spain

Eduardo J. Fernández and José M. López-de-Luzuriaga

Departamento de Química, Universidad de la Rioja, Grupo de Síntesis Química de la Rioja, UA-CSIC, Obispo Bustamante 3, E-26001 Logroño, Spain

Peter G. Jones

Institut für Anorganische und Analytische Chemie der Technischen Universität, Postfach 3329, D-38023 Braunschweig, Germany

Markus Teichert

Institut für Anorganische und Analytische Chemie der Universität, Tammannstrasse 4, D-37077, Göttingen, Germany

Miguel Monge,‡ Pekka Pyykkö,*,§ and Nino Runeberg

Department of Chemistry, University of Helsinki, P.O. Box 55 (A. I. Virtasen aukio 1), FIN-00014 Helsinki, Finland

Martin Schütz and Hans-Joachim Werner

Institut für Theoretische Chemie, Universität Stuttgart, Pfaffenwaldring 55, D-70569 Stuttgart, Germany

Received April 13, 2000

The reaction between thioether phosphine gold(I) precursors such as $[AuCl(Ph_2PCH_2SPh)]$, **1**, or $[Au(Ph_2PCH_2SPh)_2]CF_3SO_3$ and $PdCl_2(NCPh)_2$ affords the new compounds $[\{AuCl(Ph_2PCH_2SPh)\}_2PdCl_2]$, **2**, and $[AuPdCl_2(Ph_2PCH_2SPh)_2]CF_3SO_3$, **3**. The crystal structure of complex **2** has the sterically unhindered Pd(II) and Au(I) at a distance of 314 pm. Quasirelativistic pseudopotential calculations on $[AuPdCl_3(PH_2CH_2SH)(SH_2)]$ models give short Au−Pd distances at the second-order Møller−Plesset (MP2) level and long Au−Pd distances at Hartree−Fock (HF) level. A detailed analysis of the Au−Pd interaction shows dominant dispersion, some ionic contributions, and no net charge transfer between the metals.

Introduction

Although two closed-shell metal cations with the same charge would normally be expected to repel each other, evidence has been obtained for an entire family of cation−cation interactions in d^{10} or s^2 systems.[1] This attraction is now shown to originate from dispersion (van der Waals) interactions. It is comparable in strength with typical hydrogen bonds, and it is especially strengthened by relativistic effects for heavy elements such as gold.[2−4] Also, because of the large crystal-field splitting, d^8 ions are, in a sense, closed-shell atoms and can be involved in similar attractions.

Regarding d^8-d^{10} systems, a number of structurally characterized complexes in which metallophilic attraction appears are known[5−16] (see Table 1), but to the best of our knowledge,

† E-mail: alaguna@posta.unizar.es.

‡ Present and permanent address: Departamento de Química, Universidad de La Rioja.

§ E-mail: pekka.pyykko@helsinki.fi.

(1) Pyykkö, P. *Chem. Rev.* **1997**, *97*, 597−636.

(2) Pyykkö, P.; Zhao, Y.-F. *Angew. Chem., Int. Ed. Engl.* **1991**, *30*, 604−605.

(3) Pyykkö, P.; Li, J. *Chem. Phys. Lett.* **1992**, *197*, 586−590.

(4) Pyykkö, P.; Li, J. *Inorg. Chem.* **1993**, *32*, 2630−2634.

(5) Jarvis, J. A. J.; Johnson, A.; Puddephatt, R. J. *J. Chem. Soc., Chem. Commun*. **1973**, 373−374.

(6) Canales, F.; Gimeno, M. C.; Laguna, A. *Organometallics* **1996**, *15*, 3412−3415.

(7) Yamaguchi, T.; Yamazaki, F.; Ito, T. *J. Chem. Soc., Dalton Trans.* **1999**, 273−264.

(8) Albinati, A.; Lehner, H.; Venanzi, L. M.; Wolfer, M. *Inorg. Chem.* **1987**, *26*, 3933−3939.

(9) Yip, H. K.; Lin, H. M.; Wang, Y.; Che, C. M. *J. Chem. Soc., Dalton Trans.* **1993**, 2939−2944.

(10) Balch, A. L.; Nagle, J. K.; Oram, D. E.; Reedy, P. E., Jr. *J. Am. Chem. Soc.* **1988**, *110*, 454−462.

10.1021/ic000420p CCC: $19.00
Published on Web 09/21/2000

Table 1. Selected M−M′ Distances for Some d^{10}−d^8 Systems

compound	M···M′ distance (pm)	ref
$[Au^{I}Au^{III}(Me)_2(PMe_3)_2(C_4F_6)]$	331	5
$[S(Au^{I}_2dppf)\{Au^{III}(C_6F_5)_3\}_2]^a$	353, 391	6
$Ag_2[Pt(ox)_2]\cdot 2H_2O^b$	294	7
$[Ag(H_2O)_2][Ag_2(CF_3SO_3)_4][Pt(acac)_2]_2{}^c$	281	7
$[AuPt(C_6F_5)(H)(PEt_3)_2(PPh_3)]CF_3SO_3$	271	8
$[AuPt(CCPh)_2(dppm)_2]PF_6{}^d$	291	9
$[AuIr_2Cl_2(CO)_2(dppmpa)_2]BPh_4{}^e$	301, 306	10
$[AuIr(H)(CO)(PPh_3)_4]PF_6$	266	11
$[AuIrCl(CO)(dppm)_2]PF_6{}^d$	299	12
$[Au_2IrCl(CO)(dppmpa)_2](PF_6)_2{}^e$	298, 302, 301, 301	13
$[Au_3IrCl_3(CO)(dppmpp)_2]PF_6{}^f$	312	14
$[AuRh(dppmpy)_2]BF_4{}^g$	285	15
$[Au_2RhCl(CO)(dppmpa)](PF_6)_2{}^e$	300, 307, 303, 303	16

[a] dppf = bis(diphenylphosphino)ferrocene. [b] ox = oxalate. [c] acac = acetylacetonate. [d] dppm = bis(diphenylphosphino)methane. [e] dppmpa = bis(diphenylphosphinomethyl)phenylarsine. [f] dppmpp = bis(diphenylphosphinomethyl)phenylphosphine. [g] dppmpy = bis(diphenylphosphinomethyl)pyridine.

although heterometallic gold−palladium complexes have been characterized,[17] no previous examples of Au(I)···Pd(II) interactions have been reported.

As is known, the nature of intermetallic interactions can be studied by comparing Hartree−Fock (HF) and second-order Møller−Plesset (MP2) levels of theory for a given model system. Thus, when dispersion interactions are present, the intermetallic distance is shortened going from the HF to the MP2 level, where electronic correlation is included. Moreover, a more detailed analysis can be performed using the local orbital MP2 approach.[18−22] Such an analysis is particularly interesting because the role of "charge transfer" mechanisms in heteroatomic metallophilic interactions can be studied. Valid conclusions can only be reached if the theoretical calculations are in accordance with the experimental results.

As often observed, asymmetric bidentate ligands allow the synthesis of heterometallic complexes. Thus, when Ph_2PCH_2-SPh is employed, both homopolynuclear[23] and heteropolynuclear complexes[24,25] can be synthesized by exploiting the different donor properties of phosphorus and sulfur atoms present in the ligand. In this sense, two different structural arrangements can be at least proposed: on one hand, the more common dimetallic dimers, in which the intermetallic attraction is sterically imposed[23,25] and, on the other hand, the open-chain structural disposition in which the interaction between the metals, if it appears, is not sterically imposed.[25]

We report in this paper the synthesis of new heterometallic Au−Pd species in which nonimposed intermetallic interactions are present. We have also carried out ab initio calculations on simplified model systems. Further aspects are the short Au(I)−C distances between the gold and the thioether aromatic ring, found here for $[AuCl(Ph_2PCH_2SPh)]$, **1**. We here include a theoretical study for a $[ClAu(PH_2CH_2SPh)]$ model.

Methods

1. Experimental. 1.1. Instrumentation. C, H, S analyses were carried out with a Perkin-Elmer 240C microanalyzer. Mass spectra were recorded on a VG Autospec using the liquid secondary ion mass spectrometry (LSIMS) techniques and nitrobenzyl alcohol as matrix. ^1H and $^{31}P\{^1H\}$ NMR spectra were recorded on a Bruker ARX 300 in $CDCl_3$. Chemical shifts are quoted relative to $SiMe_4$ (^1H, external) and H_3PO_4 (85%) (^{31}P, external).

1.2. Solvent and Reagent Pretreatment. Dichloromethane was distilled from CaH_2 and diethyl ether from sodium, under nitrogen atmosphere. $[AuCl(Ph_2PCH_2SPh)]$ and $[Au(Ph_2PCH_2SPh)_2]CF_3SO_3$ were prepared according to reported literature methods.[23,25] $[PdCl_2(NCPh)_2]$ was purchased from Aldrich and used as received.

1.3. Synthesis of $[\{AuCl(Ph_2PCH_2SPh)\}_2PdCl_2]$ (2). To a dichloromethane solution (20 mL) of $[AuCl(Ph_2PCH_2SPh)]$ (0.2 mmol, 0.108 g) under N_2, $[PdCl_2(NCPh)_2]$ (0.1 mmol, 0.038 g) was added. The resulting orange solution was stirred for 1 h. Evaporation of the solvent to ca. 5 mL and addition of diethyl ether (20 mL) gave complex **2** as an orange solid. Yield: 83%. LSIMS: $[M - Cl]^+$ at m/z = 1223 (15%). Anal. Calcd for $C_{38}H_{34}Au_2Cl_4P_2PdS_2$: C, 36.2; H, 2.7; S, 5.1. Found: C, 36.2; H, 2.7; S, 4.9. $^{31}P\{^1H\}$ NMR ($CDCl_3$), (292 K), δ: 23.6 (s). ^1H NMR ($CDCl_3$), (292 K), δ: 7.80−7.25 [m, 30H, Ph], 4.50 [m, 4H, CH_2]. $^{31}P\{^1H\}$ NMR ($CDCl_3$), (223 K), δ: 23.3 [s, 1P], 23.2 [s, 1P]. ^1H NMR ($CDCl_3$), (223 K), δ: 7.75−7.25 [m, 30H, Ph], 4.91 [m, 2H, CH_2], 4.13 [m, 2H, CH_2].

1.4. Synthesis of $[AuPdCl_2(Ph_2PCH_2SPh)_2]CF_3SO_3$ (3). To a dichloromethane solution (20 mL) of $[Au(Ph_2PCH_2SPh)_2]CF_3SO_3$ (0.2 mmol, 0.192 g) under N_2, $[PdCl_2(NCPh)_2]$ (0.2 mmol, 0.076 g) was added. After 1 h the resulting orange solution was evaporated to ca. 5 mL. Addition of diethyl ether (20 mL) led to precipitation of complex **3** as an orange solid. Yield: 65%. LSIMS: $[M]^+$ at m/z = 991 (15%). Anal. Calcd for $C_{39}H_{34}AuCl_2F_3O_3P_2PdS_3$: C, 41.1; H, 3.0; S, 8.4. Found: C, 40.8; H, 2.9; S, 8.3. $^{31}P\{^1H\}$ NMR ($CDCl_3$), δ: 33.4 (s). ^1H NMR ($CDCl_3$), δ: 7.89−7.24 [m, 30H, Ph], 4.70 [m, 4H, CH_2].

2. Crystal Structure Determinations. The crystals were mounted in inert oil on glass fibers and transferred to the cold gas stream of a Siemens P4 (**1**) or Stoe-Siemens-Huber four-circle (**2**) diffractometers. Data were collected using monochromated Mo Kα radiation (λ = 0.710 73 Å). Scan type ω (**1**) or φ scans (**2**) were used. Absorption correction was applied on the basis of ψ scans for **1**, whereas for **2** semiempirical absorption correction was used. The structures were solved by Patterson (**1**) or direct methods (**2**) and refined on F^2 using the program SHELXL-97.[26] All non-hydrogen atoms were refined anisotropically except for solvent. Hydrogen atoms were included using a riding model. Further details of the data collection are given in Table 8. *Special details of refinement*: Complex **2** crystallizes with two molecules of dichloromethane. One of them is disordered over an inversion center. Residual electron density in the regions of some phenyl rings may indicate slight disorder.

3. Gaussian 98 Calculations. The Gaussian 98 package was used.[27] The basis sets and pseudopotentials (PP) used in the production runs are given in Table 2. The 19-valence-electron (VE) quasirelativistic (QR) pseudopotential of Andrae[28] or the 11-VE "LANL1DZ" PP[29] were employed for gold. The palladium atom was treated by an 18-VE

(11) Luke, M. A.; Mingos, D. M. P.; Sherman, D. J.; Wardle, R. W. M. *Transition Met. Chem.* **1987**, *12*, 37−41.
(12) Balch, A. L.; Catalano, V. J.; Olmstead, M. M. *Inorg. Chem.* **1990**, *29*, 585−586.
(13) Balch, A. L.; Catalano, V. J.; Olmstead, M. M. *J. Am. Chem. Soc.* **1990**, *110*, 2010−2011.
(14) Balch, A. L.; Catalano, V. J.; Noll, B. C.; Olmstead, M. M. *J. Am. Chem. Soc.* **1990**, *112*, 7558−7566.
(15) McNair, R. J.; Nilsson, P. V.; Pignolet, L. H. *Inorg. Chem.* **1985**, *24*, 1935−1939.
(16) Balch, A. L.; Fung, E. Y.; Olmstead, M. M. *Inorg. Chem.* **1990**, *29*, 3203−3207.
(17) Chiffey, A. F.; Evans, J.; Levason, W.; Webster, M. *Polyhedron* **1996**, *15*, 591−596.
(18) Pulay, P. *Chem. Phys. Lett.* **1983**, *100*, 151−154.
(19) Saebø, S.; Pulay, P. *Annu. Rev. Phys. Chem.* **1993**, *44*, 213−236.
(20) Hampel, C.; Werner, H.-J. *J. Chem. Phys.* **1996**, *104*, 6286−6297.
(21) Schütz, M.; Hetzer, G.; Werner, H.-J. *J. Chem. Phys.* **1999**, *111*, 5691−5705.
(22) Runeberg, N.; Schütz, M.; Werner, H.-J. *J. Chem. Phys.* **1999**, *110*, 7210−7215.
(23) Fernández, E. J.; López-de-Luzuriaga, J. M.; Monge, M.; Rodríguez, M. A.; Crespo, O.; Gimeno, M. C.; Laguna, A.; Jones, P. G. *Inorg. Chem.* **1998**, *37*, 6002−6006.
(24) Sanger, A. R. *Can. J. Chem.* **1983**, *61*, 2214−2219.
(25) Fernández, E. J.; López-de-Luzuriaga, J. M.; Monge, M.; Rodríguez, M. A.; Crespo, O.; Gimeno, M. C.; Laguna, A.; Jones, P. G. *Chem.*−*Eur. J.* **2000**, *6*, 636−644.
(26) Sheldrick, G. M. *SHELXL-97. A program for Crystal Structure Refinement*; University of Göttingen: Göttingen, Germany.

Table 2. Selected Bond Lengths [Å] and Angles [deg] for Compound **1**

Au−P	2.2313(13)	P−C(1)	1.824(5)
Au−Cl	2.2977(12)	S−C(31)	1.776(5)
P−C(21)	1.817(5)	S−C(1)	1.824(5)
P−C(11)	1.821(5)		
P−Au−Cl	177.49(5)	C(11)−P−Au	114.2(2)
C(21)−P−C(11)	104.1(2)	C(1)−P−Au	113.5(2)
C(21)−P−C(1)	105.6(2)	C(31)−S−C(1)	103.1(2)
C(11)−P−C(1)	104.8(2)	P−C(1)−S	113.5(3)
C(21)−P−Au	113.7(2)		

Stuttgart PP[28] or the 10-VE “LANL1DZ” PP.[29] As previously described, two f-type polarization functions for Cu, Ag, and Au are desirable for the correct description of the interaction energy. We have studied their influence in our heterodimetallic gold−palladium model.[30] For gold the f exponents are 0.2 and 1.19 and for palladium 0.25 and 1.48. The diffuse one is required for describing the metallophilic attraction and the compact one for describing the covalent bonds.

The atoms P, S, and Cl were treated by “LANL1DZ” pseudopotentials,[29] including only the valence electrons for each atom in the $[AuPdCl_3(PH_2CH_2SH)(SH_2)]$ model. In the model $[AuCl(PH_2CH_2SPh)]$ pseudopotentials from ref 31 were used. For these atoms, the double-ζ basis sets of “LANL1DZ”[41] were used, augmented by p-type and d-type polarization functions in cases 3 and 4, for the gold−palladium model[29] and double-ζ basis sets from ref 31 augmented by p-type and d-type polarization functions[32] in the $[AuCl(PH_2CH_2SPh)]$ model. For C atoms we used “LANL1DZ” basis sets[29] with or without p- and d-type polarization functions for the gold−palladium model and basis sets and pseudopotentials from ref 31 plus p- and d-type polarization functions for the chlorogold thioetherphosphine model. For the H atoms, we used

(27) Frisch, M. J.; Trucks, G. W.; Schlegel, H. B.; Scuseria, G. E.; Robb, M. A.; Cheeseman, J. R.; Zakrzewski, V. G.; Montgomery, J. A., Jr.; Stratmann, R. E.; Burant, J. C.; Dapprich, S.; Millam, J. M.; Daniels, A. D.; Kudin, K. N.; Strain, M. C.; Farkas, O.; Tomasi, J.; Barone, V.; Cossi, M.; Cammi, R.; Mennucci, B.; Pomelli, C.; Adamo, C.; Clifford, S.; Ochterski, J.; Petersson, G. A.; Ayala, P. Y.; Cui, Q.; Morokuma, K.; Malick, D. K.; Rabuck, A. D.; Raghavachari, K.; Foresman, J. B.; Cioslowski, J.; Ortiz, J. V.; Stefanov, B. B.; Liu, G.; Liashenko, A.; Piskorz, P.; Komaromi, I.; Gomperts, R.; Martin, R. L.; Fox, D. J.; Keith, T.; Al-Laham, M. A.; Peng, C. Y.; Nanayakkara, A.; Gonzalez, C.; Challacombe, M.; Gill, P. M. W.; Johnson, B. G.; Chen, W.; Wong, M. W.; Andres, J. L.; Head-Gordon, M.; Replogle, E. S.; Pople, J. A. *Gaussian 98*; Gaussian, Inc.: Pittsburgh, PA, 1998.
(28) Andrae, D.; Häusserman, U.; Dolg, M.; Stoll, H.; Preuss, H. *Theor. Chim. Acta* **1990**, *77*, 123−141.
(29) Hay, P. J.; Wadt, W. R. *J. Chem. Phys.* **1985**, *82*, 270−283.
(30) Pyykkö, P.; Runeberg, N.; Mendizabal, F. *Chem.*−*Eur. J.* **1997**, *3*, 1451−1457.
(31) Bergner, A.; Dolg, M.; Küchle, W.; Stoll, H.; Preuss, H. *Mol. Phys.* **1993**, *80*, 1431−1441.
(32) Huzinaga, S. *Gaussian Basis Sets for Molecular Calculations*; Elsevier: Amsterdam, 1984; p 16.
(33) Huzinaga, S. *J. Chem. Phys.* **1965**, *42*, 1293−1302.
(34) MOLPRO is a package of ab initio programs written by the following: Werner, H.-J.; Knowles, P. J. Contributions are from the following: Amos, R. D.; Berning, A.; Cooper, D. L.; Deegan, M. J. O.; Dobbyn, A. J.; Eckert, F.; Hampel, C.; Leininger, T.; Lindh, R.; Lloyd, A. W.; Meyer, W.; Mura, M. E.; Nicklass, A.; Palmieri, P.; Peterson, K.; Pitzer, R.; Pulay, P.; Rauhut, G.; Schütz, M.; Stoll, H.; Stone, A. J.; Thorsteinsson, T.
(35) Woon, D. E.; Dunning, T. H., Jr. *J. Chem. Phys.* **1993**, *98*, 1358−1371.
(36) Dunning, T. H., Jr. *J. Chem. Phys.* **1989**, *90*, 1007−1023.
(37) Pipek, J.; Mezey, P. G. *J. Chem. Phys.* **1989**, *90*, 4916−4926.
(38) Jones, P. G.; Freire Erdbrügger, C.; Hohbein, R.; Schwarzmann, E. *Acta Crystallogr.* **1988**, *C 44*, 1302−1303.
(39) (a) Aullon, G.; Bellamy, D.; Brammer, L.; Bruton, E. A.; Orpen, A. G. *J. Chem. Soc., Chem. Commun.* **1998**, 653−654. (b) Aakeroy, C. B.; Evans, T. A.; Seddon, K. R.; Palinko, Y. *New J. Chem.* **1998**, *23*, 145−152. (c) Freytag, M.; Jones, P. G. *Chem. Commun.* **2000**, 277−278.
(40) Jones, P. G.; Ahrens, B. *J. Chem. Soc., Chem Commun.* **1998**, 2307−2308.
(41) Ito, L. N.; Felicissimo, A. M. P.; Pignolet, L. H. *Inorg. Chem.* **1991**, *30*, 988−994.

Scheme 1. Synthetic Routes to the Gold−Palladium Complexes[a]

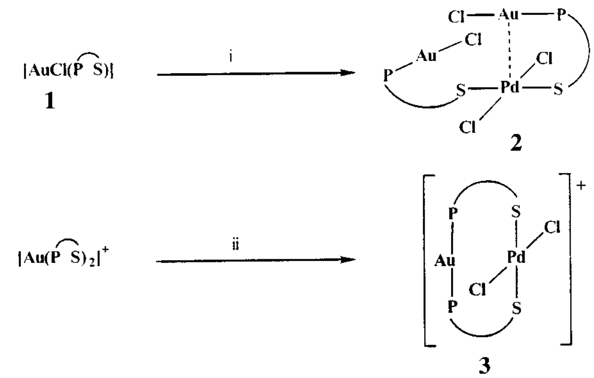

[a] (i) $^1/_2[PdCl_2(NCPh)_2]$; (ii) $[PdCl_2(NCPh)_2]$.

“LANL1DZ” basis sets[29] with or without one p-type polarization function for the gold−palladium model and a double-ζ plus one p-type polarization function was used for the chlorogold thioetherphosphine model[33] (see Tables 4 and 5).

We have optimized the structures without assuming any symmetry and keeping the bond distances frozen to experimental values for both $[AuPdCl_3(PH_2CH_2SH)(SH_2)]$ and $[AuCl(PH_2CH_2SPh)]$ models, at the Hartree−Fock and MP2 levels. We study the intramolecular interactions using the difference between the Au−Pd distances and Cl−Au−P angles in the former model and between Au−C distances and Cl−Au−P angles in the latter one, calculated at HF and MP2 levels for each model. This gives us an idea of the contribution of the electronic correlation to the intramolecular contacts for this system.

4. Localized MP2 Calculations. All LMP2 calculations on the *trans*-$H_2Pd(PH_3)_2 \cdots HAuPH_3$ system have been done as implemented in the MOLPRO program package.[34] For the metals, the PPs and basis sets from Stuttgart[27] augmented with two f-functions were used (see Table 4). Correlation-consistent valence double-ζ (cc-pVDZ) basis sets were used for P and H.[35,36] The monomers were optimized separately and kept frozen in the dimer calculations. The LMOs were obtained through a Pipek−Mezey localization procedure.[37] The orbital domains are determined at large distances and kept fixed for all other distances.

Results and Discussion

1. Syntheses. As we previously reported, when an asymmetric bidentate ligand like Ph_2PCH_2SPh is employed, the donor atoms can selectively coordinate to different metal centers.[25] The use of this bidentate ligand allows, in the first step, the selective coordination of phosphorus to gold(I), leaving the sulfur atom as a potentially coordinative heteroatom. Reaction of $[AuCl(Ph_2PCH_2SPh)]$[23] (**1**) with $[PdCl_2(NCPh)_2]$ in a 2:1 molar ratio affords the substitution of the weakly coordinated benzonitrile ligands, forming the trinuclear complex $[\{AuCl(Ph_2PCH_2SPh)\}_2PdCl_2]$ (**2**) (see Scheme 1) in which the coordination of the palladium center is expected to be at the sulfur atoms of the two chlorogold units. This compound is an orange solid stable to air and moisture at room temperature. The $^{31}P\{^1H\}$ NMR shows at room temperature at 23.6 ppm a singlet whose chemical shift is not far from the corresponding one for the gold starting material. The signal splits into two of the same intensity when the temperature is decreased to 223 K. Nevertheless, their proximity (23.3 and 23.2 ppm) seems to indicate a different magnetic environment that is not due to the coordination of the phosphorus atoms of the ligands to different metal centers (gold and palladium). An estimation of the activation barrier of the gold−palladium interaction in compound **2** from the coalescence parameters ($^{31}P\{^1H\}$ NMR) gives a $\Delta G^{\ddagger}$ value of ca. 53.7 ± 0.2 kJ mol^{-1} (coalescence temperature at 249 K). In addition, in the ^1H NMR spectrum the same situation appears

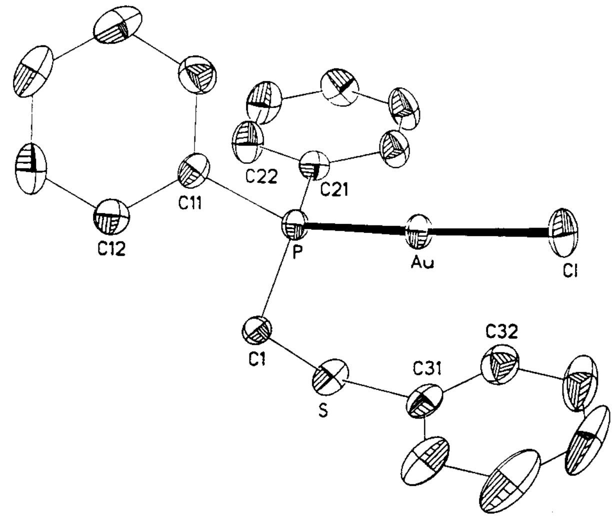

Figure 1. Molecule of **1** in the crystal with the atom numbering scheme. Hydrogens are omitted for clarity. Radii are arbitrary.

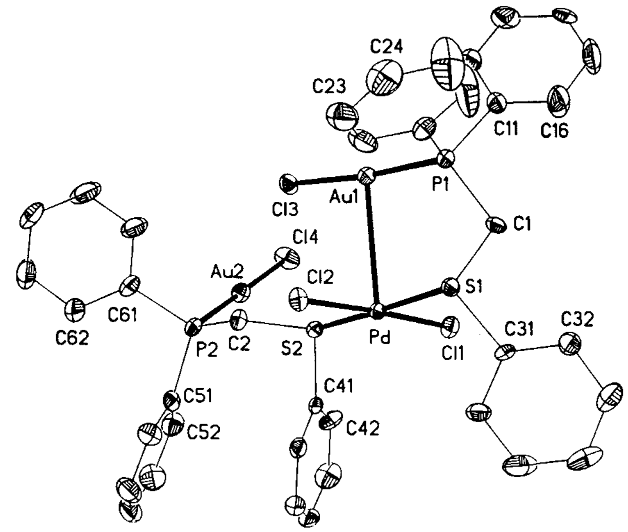

Figure 2. Molecule of **2** in the crystal with the atom numbering scheme. Hydrogens are omitted for clarity. Radii are arbitrary.

and one signal placed at 4.50 ppm at room temperature, because of the CH_2 groups, splits into two signals centered at 4.91 and 4.13 ppm at 223 K assigned to each methylenic group of the inequivalent ligands. In this case the activation barrier gives a $\Delta G^{\ddagger}$ value of ca. 53.5 $\pm$ 0.2 kJ mol^{-1} (coalescence temperature at 278 K). These values are higher than the one obtained theoretically (see below) perhaps because of the simplification of the theoretical model (no bridging group, chlorines replaced by hydrogens, simplified phosphines on Au, thioethers on Pd replaced by phosphines). The mass spectrum (LSIMS+) shows in this case the $[M - Cl]^+$ peak at 1223 (15%) with a theoretical isotopic distribution that matches the experimental one.

When the starting gold(I) complex is the derivative $[Au(Ph_2PCH_2SPh)_2]CF_3SO_3$,[25] the reaction with $[PdCl_2(NCPh)_2]$ (1:1 molar ratio) gives rise to the dinuclear complex $[AuPdCl_2(Ph_2PCH_2SPh)_2]CF_3SO_3$ (**3**) (see Scheme 1), in which the phosphinothioether ligands are bonded to the gold center through their phosphorus atoms and to the palladium through the sulfur centers. The complex is orange and is an air- and moisture-stable solid at room temperature. The formulation agrees with the data obtained from the $^{31}P\{^1H\}$ NMR experiment because only one signal at 33.4 ppm is observed, indicating the equivalence of both phosphorus atoms and that the chemical shift is in the same range as in the starting material (39.7 ppm). The mass spectrum (LSIMS+) shows the molecular peak at 991 (15%) with an isotopic distribution in accordance with the theoretical one. Other analytical data also agree with this formulation (see experimental section).

The crystal structures of complexes **1** and **2** were unequivocally determined by X-ray diffraction studies. In the mononuclear compound **1** (Figure 1) the metallic atom displays a slightly distorted linear geometry (P−Au−Cl = 177.49(5)°). The distances Au−Cl = 2.2977(12) Å and Au−P = 2.2313(13) Å are about the same as others found in chloro(phosphine)gold(I) complexes such as $[AuCl(PPhFc_2)]$[38] (Fc = $(\eta^5\text{-}C_5H_5)Fe(\eta^5\text{-}C_5H_4)$) (2.289(2) and 2.234(2) Å, respectively). The structure displays several short contacts such as weak intermolecular Au···Au contacts of 4.140(1) Å (operator $-x$, $1-y$, $1-z$) and an intramolecular H26···Au contact of 3.01 Å. Short Au(1)−C(31) and Au(1)−C(32) distances of 3.375 and 3.577 Å, respectively, indicate a weak η^2 interaction between the gold center and the thioether aromatic ring. Rather stronger secondary interactions are probably indicated by the H···Cl contacts H1A···Cl (x, $1+y$, z) and H1B···Cl ($-x$, $1-y$, $1-z$), 2.68 and 2.67 Å, respectively. These are of acceptable linearity (C−H···Cl = 158, 162°) and may be considered as weak hydrogen bonds.[39] The methylene hydrogen atoms should be the most acidic and thus most likely to act as H bond donors (see our recent studies of metal complexes of dppm derivatives).[40] A selection of bond lengths and angles is shown in Table 2.

Complex **2** is a trinuclear derivative (Figure 2) in which the palladium center displays square planar geometry (angles Cl−Pd−S range from 84.18(8)° to 95.74(8)°). The palladium atom lies less than 0.001 Å out of the plane defined by S1, S2, C11, and C12, despite its interaction with the gold atom of 3.1418(8) Å. The gold centers exhibit almost linear geometries. The major distortion from the ideal linear structure is found for Au(1) (P(1)−Au(1)−Cl(3) = 174.88(8)°, P(2)−Au(2)−Cl(4) = 177.83(9)°) and arises from the observed Pd−Au(1) contact. Such Pd(II)···Au(I) interactions had not been reported before and cannot be imposed by steric demands taking into account the long chain of the ligand. A search in the Cambridge Structural Database for Pd−Au bonds gave rise to nine compounds. Most of them consist of cores in which a palladium center is surrounded by "$Au(PR_3)$" fragments (PR_3 = tertiary phosphine) in which the Au−Pd bond distance averages are 2.673 Å $[Au_8Pd(PPh_3)_8(CO)](NO_3)_2$,[41] 2.709 Å $[Au_8Pd(PPh_3)_5\{P(OMe)_3\}_3](NO_3)_2$,[41] or 2.618 Å $[Au_8Pd(PPh_3)_8](NO_3)_2$.[42] The Au−P bond lengths of 2.237(2) and 2.234(2) Å and the Au−Cl bond lengths of 2.295(2) and 2.308(2) Å are about the same as those found in **1**. The distances corresponding to Pd−Cl of 2.292(2), 2.312(2) Å and Pd−S of 2.310(2)), 2.333(2) Å may be compared with those in other *trans*-$[PdCl_2L_2]$ complexes (L = 2,3-dihydrobenzo[*b*]thiophene,[43] SP^iBu_3,[44] or PhS−CH_2−SPh[45]). The approximately linear groups P1−Au1−C13 and S1−Pd−S2 are almost eclipsed, with torsion angle P1−Au1−Pd−S1 of 8°. A selection of bond lengths and angles is shown in Table 3.

2. Theoretical. 2.1. Metallophilic Attraction: HF versus MP2. To keep the computational costs feasible, the experimen-

(42) Ito, L. N.; Johnson, B. J.; Muetig, A. M.; Pignolet, L. H. *Inorg. Chem.* **1989**, *28*, 2026−2028.
(43) Clark, P. D.; Fait, J. F.; Jones, C. G.; Kirk, M. J. *Can. J. Chem.* **1991**, *69*, 590−598.
(44) Richardson, M. F. *Acta Crystallogr.* **1985**, *C41*, 57−58.
(45) Chiffey, A. F.; Evans, J.; Levason, W.; Webster, M. *J. Chem. Soc., Dalton Trans.* **1994**, 2835−2840.

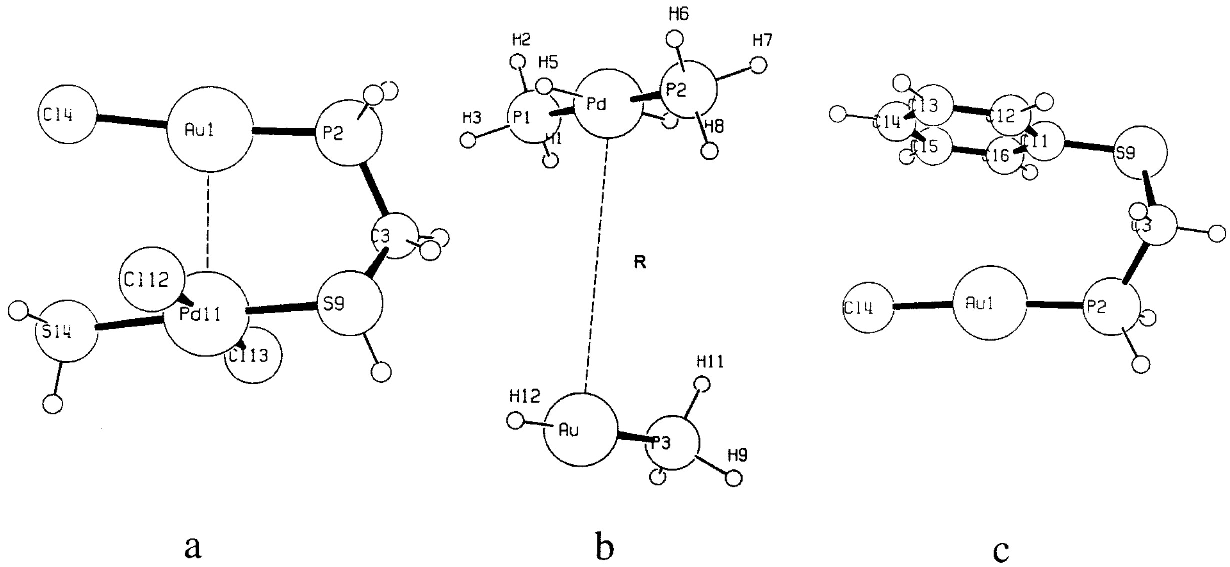

Figure 3. Assumed structures of the gold−palladium models: (a) $[AuPdCl_3(PH_2CH_2SH)(SH_2)]$, **2a**; (b) *trans*-$[PdH_2(PH_3)_2][HAuPH_3]$, **2b**; (c) chlorogold phosphine model $[AuCl(PH_2CH_2S(C_6H_5)]$, **1a**.

Table 3. Selected Bond Lengths [Å] and Angles [deg] for Compound **2**

Au(1)−P(1)	2.237(2)	P(1)−C(11)	1.805(9)
Au(1)−Cl(3)	2.308(2)	P(1)−C(1)	1.834(8)
Au(1)−Pd	3.1418(8)	P(1)−C(21)	1.835(9)
Au(2)−P(2)	2.234(2)	P(2)−C(61)	1.812(9)
Au(2)−Cl(4)	2.295(2)	P(2)−C(51)	1.814(9)
Pd−Cl(1)	2.299(2)	P(2)−C(2)	1.841(8)
Pd−S(29)	2.310(2)	S(1)−C(31)	1.792(8)
Pd−Cl(2)	2.312(2)	S(1)−C(1)	1.825(8)
Pd−S(1)	2.333(2)	S(2)−C(41)	1.786(8)
		S(2)−C(2)	1.813(8)
P(1)−Au(1)−Cl(3)	174.88(8)	C(61)−P(2)−C(51)	107.3(4)
P(2)−Au(2)−Cl(4)	177.73(9)	C(61)−P(2)−C(2)	101.9(4)
Cl(1)−Pd−S(2)	84.18(8)	C(51)−P(2)−C(2)	107.9(4)
Cl(1)−Pd−Cl(2)	177.26(8)	C(61)−P(2)−Au(2)	113.9(3)
S(2)−Pd−Cl(2)	95.74(8)	C(51)−P(2)−Au(2)	116.0(3)
Cl(1)−Pd−S(1)	91.99(8)	C(2)−P(2)−Au(2)	108.8(3)
S(2)−Pd−S(1)	175.23(8)	C(31)−S(1)−C(1)	102.8(4)
Cl(2)−Pd−S(1)	88.22(8)	C(31)−S(1)−Pd	105.5(3)
C(11)−P(1)−C(1)	104.2(4)	C(1)−S(1)−Pd	104.3(3)
C(11)−P(1)−C(21)	106.3(4)	C(41)−S(2)−C(2)	100.2(4)
C(1)−P(1)−C(21)	104.2(4)	C(41)−S(2)−Pd	108.0(3)
C(11)−P(1)−Au(1)	111.6(3)	C(2)−S(2)−Pd	109.5(3)
C(1)−P(1)−Au(1)	116.0(3)	S(1)−C(1)−P(1)	109.2(4)
C(21)−P(1)−Au(1)	113.6(3)	S(2)−C(2)−P(2)	110.9(4)

tally obtained complex **2** was substituted with the simplified model system $[AuPdCl_3(PH_2CH_2SH)(SH_2)]$, **2a** (Figure 3a). This model system was studied at four different levels of pseudopotentials and basis sets, as explained in Tables 4 and 5. The results for **2a** are shown in Table 6. Compared with experimental ones, the HF Au−Pd distances are much too large and the Cl−Au−P angles are bent outward (Cl−Au−P > 180°). The best MP2 calculation (19-VE Au, 18-VE Pd, 2f polarization functions) is case 4. That calculated Au−Pd distance of 292 pm is below the experimental value. It is known[1] that the MP2 approximation exaggerates the attraction. Furthermore, no correction could be included for the basis set superposition error (BSSE) in an intramolecular case.

If the polarization functions on main group atoms are omitted (case 2), the Au−Pd distance is lengthened by only 1 pm. Other parameters remain almost unchanged.

Going from case 4 to case 3, we exchange the small-core PP to a large-core one. Concomitantly the Au valence 6s and 6p orbitals lose their nodes. This is the third factor (in addition to MP2 and BSSE) that exaggerates the attraction, and indeed, case 3 has the shortest Au−Pd distance. Then, if all polarization functions are omitted (case 1), the Au−Pd distance is strongly increased. Because of a cancellation of this basis set error against the three other errors (MP2, BSSE, and no nodes), the result is close to experimental results.

All MP2 calculations give Cl−Au−P angles bent inward (<180°). The HF calculations give angles bent outward (>180°).

2.2. Metallophilic Attraction: Localized Orbital Treatment. Dynamical electron correlation in molecules is normally a short-range effect that decays with $1/r^6$ (dispersion energy). By employing a computational approach that uses a local orbital basis, the computational cost and BSSE can be significantly reduced. The local second-order Møller−Plesset perturbation (LMP2) theory, which is the simplest of the local correlation methods,[18−20] is analogous to the traditional MP2, but it is performed using localized occupied and local nonorthogonal virtual orbitals. The occupied localized molecular orbitals (LMO) are obtained via one of the well-established localization procedures.[37] The orbital domain [*i*] is the part of the virtual space assigned to an individual LMO (*i*) consisting of only those basis functions that are centered on the atoms involved in that particular LMO. The orbital domains [*i*] are kept orthogonal to the occupied space by projecting out the LMOs. Double excitations from an orbital pair (*ij*) are only allowed into the *pair domain* [*ij*], which is spanned by the union of the corresponding orbital domains [*i*] and [*j*]. The introduction of this physically appealing restriction in which electron pairs are only interacting in the vicinity of either electron gives rise to the significant reduction of the computational cost as well as a diminished BSSE. In the present work we have chosen *trans*-$H_2Pd(PH_3)_2\cdots HAuPH_3$ (**2b**) (Figure 3b) as an unbridged model system used in the LMP2 calculations, since it makes it possible to uniquely ascribe all local orbitals to one monomer.

The calculated interaction energy curves are shown in Figure 4. The HF curve is repulsive, while the LMP2 one is attractive. The calculated Au−Pd distance of 304 pm for our unbridged model system is fairly close to the experimental one of 314.2 pm. The interaction energy is 35 kJ/mol, a typical value for the metallophilic attraction. Note the approximations made in the model when comparing this value with the experimental ones.

Table 4. Basis Sets and Pseudopotentials (PP) Used in the Present Work

atom	PP	basis	remarks
H		LANL1DZ basis for H	$\alpha_p = 0.8$[a]
C		LANL1DZ basis for C	$\alpha_p = 0.1561$, $\alpha_d = 0.60$[a]
P	5VE-LANL1DZ[d]	LANL1DZ basis for P	$\alpha_p = 0.084$, $\alpha_d = 0.34$[a]
S	6VE-LANL1DZ[d]	LANL1DZ basis for S	$\alpha_p = 0.1017$, $\alpha_d = 0.4210$[a]
Cl	7VE-LANL1DZ[d]	LANL1DZ basis for Cl	$\alpha_p = 0.0154$, $\alpha_d = 0.514$[a]
H		cc-pVDZ/(4s1p)/[2s1p]	$\alpha_p = 0.727$[b]
P		cc-pVDZ/(12s8p1d)/[4s3p1d]	$\alpha_d = 0.373$[b]
H		(4s1p)/[2s1p][e]	$\alpha_p = 0.8$[c]
C	Bergner	(4s4p1d)/[2s2p1d]	$\alpha_p = 0.1561$, $\alpha_d = 0.60$[c]
P	Bergner	(4s4p1d)/[2s2p1d]	$\alpha_p = 0.084$, $\alpha_d = 0.34$[c]
S	Bergner	(4s5p1d)/[2s2p1d]	$\alpha_p = 0.1017$, $\alpha_d = 0.421$[c]
Cl	Bergner	(4s5p1d)/[2s2p1d]	$\alpha_p = 0.0154$, $\alpha_d = 0.514$[c]
Pd	10VE-LANL1DZ	LANL1DZ basis for Pd	$\alpha_f = 0.25, 1.48$[a]
Pd	18VE-Andrae	(8s7p6d2f)/[6s5p3d2f]	$\alpha_f = 0.25, 1.48$[a,b]
Au	11VE-LANL1DZ	LANL1DZ basis for Au	$\alpha_f = 0.2, 1.19$[a]
Au	19VE-Andrae	(8s7p6d2f)/[6s5p3d2f]	$\alpha_f = 0.2, 1.19$[a−c]

[a] Basis sets and pseudopotentials used for the Au−Pd model system **2a** with or without polarization functions. [b] Basis sets and pseudopotentials used for the Au−Pd model system **2b**; see refs 35 and 36. [c] Basis sets and pseudopotentials used for the [AuCl(PH_2CH_2SPh)] model system **1a**. [d] Reference 29. [e] Reference 33.

Table 5. Studied Cases for the Model Systems [$AuPdCl_3(PH_2CH_2SH)(SH_2)$], **2a**, and [AuCl{$PH_2CH_2S(C_6H_5)$}], **1a**

case	model	basis sets and PPs for H, C, P, S, Cl	basis sets and PPs for Au and Pd	polarization functions
1	**2a**	LANL1DZ[a]	LANL1DZ basis sets and 10-VE and 11-VE PPs[a]	no polarization functions
2	**2a**	LANL1DZ[a]	Andrae basis sets and 19-VE, 18-VE PPs[b]	2f polarization function for Au and Pd
3	**2a**	LANL1DZ[a]	LANL1DZ basis sets and 10-VE and 11-VE PPs[a]	2f for Au and Pd. p and d for C, P, S Cl. p for H
4	**2a**	LANL1DZ[a]	Andrae basis sets and 19-VE, 18-VE PPs[b]	2f for Au and Pd. p and d for C, P, S Cl. p for H
5	**1a**	basis sets and PPs from ref 31 for C, P, S, and Cl and ref 33 for H	Andrae basis sets and 19-VE, 18-VE PPs[b]	2f for Au and Pd. p and d for C, P, S Cl. p for H

[a] See ref 29. [b] See ref 28.

Table 6. Selected Experimental Structural Parameters[a] for [$Au_2Pd(Cl)_4(Ph_2PCH_2SPh)_2$], **2**, and Optimized Geometries for the [$AuPdCl_3(PH_2CH_2SH_2)(SH_2)$] Model System **2a** at MP2 and HF Levels (Distances in pm and Angles in deg)

system	case no.	method	Au−Pd distance	Cl−Au−P angle	S−Pd−S angle	P−C−S angle	P···S distance
2		expt	314.2	174.9	175.2	109.2	298.3
2a	1	HF	348.8	185.1	179.4	114.8	307.1
2a	1	MP2	309.1	175.2	175.1	112.7	303.4
2a	2	MP2	293.1	173.1	171.8	111.6	301.6
2a	3	HF	348.6	183.6	179.4	114.4	306.3
2a	3	MP2	277.9	170.2	170.0	109.6	297.8
2a	4	MP2	292.0	174.6	172.0	109.7	298.0

[a] The structure was obtained by X-ray diffraction.

A more detailed interpretation of the Au(I)···Pd(II) attraction, caused by electron correlation, is possible within the LMP2 theory. The LMP2 theory offers the possibility of decomposing the correlation energy into different classes according to different double-excitations patterns. By using *trans*-$H_2Pd(PH_3)_2$···$HAuPH_3$ (**2b**) (Figure 3b) as an unbridged model system with almost nonoverlapping monomers (M(A)···M(B)), we can uniquely ascribe every local orbital to either monomer's occupied (A,B) or virtual (A′,B′) space. This partition of the orbitals gives rise to the double-excitation classes a−g shown in Figure 5. Only classes a−e are included in the local treatment. Class f is primarily responsible for BSSE in canonical MP2 calculations, but it is excluded in LMP2, resulting in an almost BSSE-free interaction energy and equilibrium structure. The error due to the absence of the ionic class g is expected to be small.

The partitioning of the correlation contribution to the *trans*-$H_2Pd(PH_3)_2$···$HAuPH_3$ interaction energy is shown in Figure 6. The empty squares give the dispersion contribution (class b in Figure 5). The filled circles give the total ionic contribution (class d + class e in Figure 5), consisting of the two "charge-transfer" components in the directions Au → Pd (open triangle)

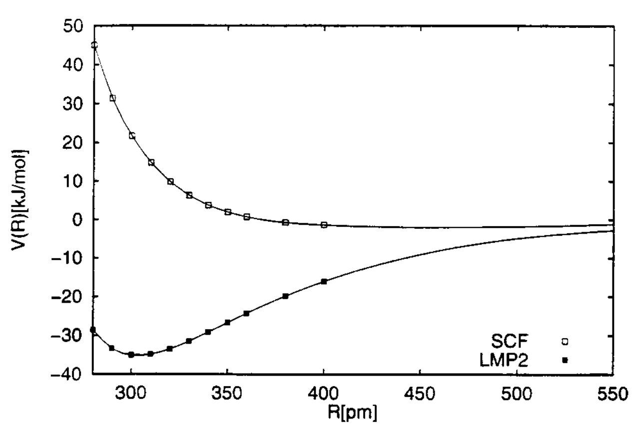

Figure 4. LMP2/cc-pVDZ interaction for *trans*-[$PdH_2(PH_3)_2$][$HAuPH_3$], **2b**.

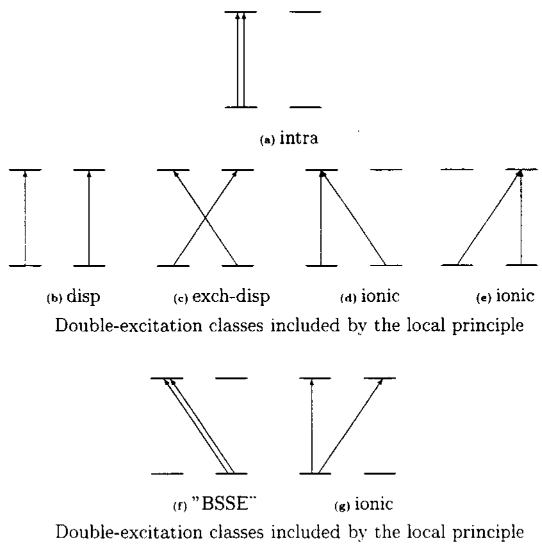

Figure 5. Different types of double excitations in a local-orbital basis.

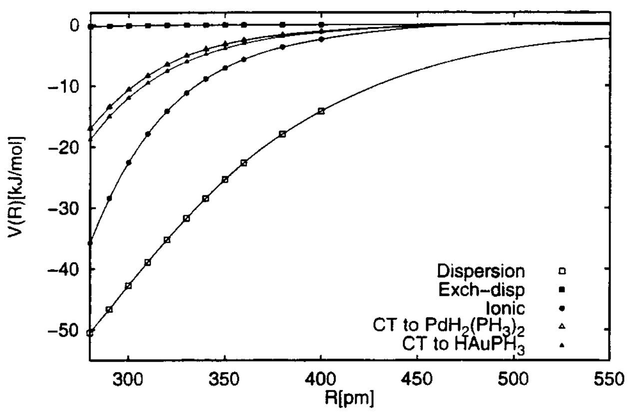

Figure 6. Components of the interaction energy for the model *trans*-$[PdH_2(PH_3)_2][HAuPH_3]$, **2b**.

Table 7. Selected Experimental Structural Parameters[a] for $[AuCl(Ph_2PCH_2SPh)]$, **1**, and Optimized Geometries for the $[AuCl(PH_2CH_2S(C_6H_5)]$ Model System **1a** at MP2 and HF Levels (Distances in pm and Angles in deg)

system	case no.	method	Au−C11 distance	Au−C12 distance	Cl−Au−P angle	P−S distance
1			337.5	357.7	177.5	305.1
1a	5	HF	404.7	368.2	179.0	302.8
1a	5	MP2	319.3	318.3	175.8	298.9

[a] The structure was obtained by X-ray diffraction.

and Pd → Au (closed triangles). Energywise, these two effects are comparable. The total ionic effect is about half of the dispersion one, or one-third of the total attraction. Recall that for $[XAuPH_3]_2$ (X = H, Cl) the ionic and dispersion contributions to V(Re) were comparable.[22] The repulsive parts of V, or minor contributions such as reduced intramolecular correlation, are not included in Figure 6.

2.3. Au(I) Aromatic Ring Interaction. The Au(I) aromatic ring interaction was studied using the model system [ClAu-(PH_2CH_2SPh)], **1a** (Figure 3c). The results are shown in Table 7. All primary bond lengths were fixed at their experimental values. All angles were optimized. At the HF level the Au−ring distance would be much too long. At the MP2 level the Au−C11 and Au−C12 distances are considerably shortened and become more equal. Recall the result of Dargel et al.[46] that a free Au^+ above C_6H_6 would prefer a bridging η^2 position.

Table 8. Details of Data Collection and Structure Refinement for Complexes **1** and **2**

	$[AuCl(Ph_2PCH_2SPh)]$	$[\{AuCl(Ph_2PCH_2SPh)\}_2-PdCl_2]\cdot 1.5\ CH_2Cl_2$
chemical formula	$C_{19}H_{17}AuClPS$	$C_{39.50}H_{37}Au_2Cl_7P_2PdS_2$
cryst habit	irregular fragment	tablet
cryst size, mm	0.40 × 0.25 × 0.20	0.25 × 0.12 × 0.05
cryst syst	monoclinic	monoclinic
space group	$P2_1/n$	$P2_1/c$
a, Å	11.896(2)	14.294(3)
b, Å	9.124(2)	13.910(3)
c, Å	16.858(2)	22.513(4)
β, deg	94.71(2)	94.40(2)
U, Å^3	1823.5(5)	4463(2)
Z	4	4
D_c, g cm^{-3}	1.970	2.063
M	540.77	1386.23
F(000)	1032	2636
temp, °C	−100	−140
$2\theta_{max}$, deg	55	52
μ(Mo Kα), cm^{-1}	84	76
transmission	0.796−0.715	0.647−0.539
no. reflns measd	4221	75135
no. unique reflns	4179	8779
R_{int}	0.0113	0.102
R [a] ($F > 4\sigma(F)$)	0.0282	0.0504
wR [b] (F^2, all reflns)	0.0593	0.094
no. reflns used	4179	8779
no. params	209	497
no. restraints	168	336
S [c]	0.872	1.180
max Δρ, e Å^{-3}	1.670	1.427

[a] $R(F) = \sum||F_o| - |F_c||/\sum|F_o|$. [b] $wR(F^2) = [\sum\{w(F_o^2 - F_c^2)^2\}/\sum\{w(F_o^2)^2\}]^{0.5}$; $w^{-1} = s^2(F_o^2) + (aP)^2 + bP$, where $P = [F_o^2 + 2F_c^2]/3$ and a and b are constants adjusted by the program. [c] $S = [\sum\{w(F_o^2 - F_c^2)^2\}/(n-p)]^{0.5}$, where n is the number of data points and p the number of parameters.

One should note, however, the large variation in Au−C distances and bond strengths: $Au^+(\eta^2)C_6H_6$ (g) has an Au−C distance (MP2, BS1) of 230 pm and an interaction energy of 229 kJ/mol.[46] In the ferrocene complex the shortest Au−C distance is 298 pm.[47] Besides, in the $[Au(PPh_3)\{P(CH_2SPh)_3\}]$ complex its unusual structure shows the three CH_2SPh arms folded back toward the metal atom, which may be due to the presence of gold(I)−aromatic rings interactions.[48] In the present **1** the shortest Au−C distance is 337 pm.

Conclusions

(1) Compound **2** contains the first known Au(I)−Pd(II) interaction. (2) Compound **1** gives a new example of an Au(I)−phenyl ring interaction. (3) Theoretical treatments of both attractions require correlation effects. (4) The main contribution to the Pd(II)−Au(I) attraction is dispersion. Charge-transfer type contributions are about half as important, but the two contributions Pd → Au and Au → Pd are energetically comparable.

Acknowledgment. This work was supported by the Spanish DGES (PB97-1010) and the U.R. API 99/B08. P. Pyykkö and N. Runeberg are supported by The Academy of Finland. The work in Stuttgart is performed under the TMR network FMRX-CT96-0088. The work in Braunschweig, Göttingen, and Stuttgart is supported by the Fonds der Chemischen Industrie.

IC000420P

(46) Dargel, T. K.; Hertwig, R. H.; Koch, W. *Mol. Phys.* **1999**, *96*, 583−591.
(47) Gimeno, M. C.; Jones, P. G.; Laguna, A.; Sarroca, C.; Calhorda, M. J.; Veiros, L. F. *Chem.*−*Eur. J.* **1998**, *4*, 2308−2314.
(48) Fuchs, S.; López-de-Luzuriaga, J. M.; Olmos, M. E.; Sladek, A.; Schmidbaur, H. *Z. Naturforsch.* **1996**, *52b*, 217−220.